EFFECTS ON SPOKE STRUCTURE OF NON-PNEUMATIC TIRES BY FINITE ELEMENT ANALYSIS

Juthanee Phromjan[1,2)] and Chakrit Suvanjumrat[1,2)*]

[1)]Laboratory of Computer Mechanic for Design (LCMD), Department of Mechanical Engineering,
Faculty of Engineering, Mahidol University, Nakhon Pathom 73170, Thailand
[2)]Department of Mechanical Engineering, Faculty of Engineering, Mahidol University,
Nakhon Pathom 73170, Thailand

ABSTRACT–Cause of the non-pneumatic tires (NPTs) which are recent manufacturing have a higher weight that increases energy consumption for driving vehicles with them. This paper then focused on their proper spoke structure. Six patterns of spoke aligning on the NPT circumference were proposed to reduce the NPT weight. The finite element analysis (FEA) of the NPTs based on static and dynamic approaches was performed to study the spoke reduction effects. One pattern of spoke alignments was experimentally performed in the stiffness testing. The tested NPT had been prepared by cutting spokes of the original NPT with the water jet cutting technique. The experimental results then confirmed the accuracy of FEA in reducing the NPT's weight. It found that the average error of FEA was less than 0.30 %. Therefore, the uniform spoke alignment on the NPT circumference had been carried out to study the effect of spoke numbers on reducing NPT weight by FEA. In advance of NPT design and manufacture with optimal weight, the vertical stiffness equation of this NPT was proposed by two variables, the number, and thickness of the spoke. Furthermore, the stress happening on the spokes was represented as a function to evaluate the NPT performance during operation.

KEY WORDS : Finite element method, Non-pneumatic tire, Spoke, Weight

1. INTRODUCTION

Tires are the necessary mobility part for ground vehicles. In our modern world, conventional pneumatic tires supply to use extensively. However, vehicle driving with these tires has many disadvantages. For example, it can flat easily, which is the cause of vehicle immobilization. Moreover, its carrying load is most dependent on inflation pressure, which is not suitable in some applications such as construction and agriculture. The development of non-pneumatic tires (NPT) to overcome the disadvantages of pneumatic tires occurred recently. The basic design concept of NPT is a combination of a shear band and a spoke structure. They have similar functions as the belt and air pressure in a pneumatic tire. The advantage of the spoke structure is its high out-of-plane stiffness, while the in-plane properties are much weaker to evoke high in-plane deformation (Bitzer, 1997; Ju *et al*., 2012). The lateral stiffness, which affected the handling and cornering of NPTs, could be independently developed with the vertical stiffness, which was affected the riding comfort and load carrying capacity (Rhyne and Cron, 2006). Due to the

spokes created to support the vehicle's load and distribute impact force. Therefore spokes could also replace the carcass and sidewall of the pneumatic tires (Sim *et al*., 2021). NPT's spoke is produced from polyurethane (PU) material, which has sturdiness, resilience, and impact resistance as outstanding features. Therefore the spoke is tough to damage from potholes and poor road conditions. Consequently, many previous studies of NPT regarded to improve the spoke structure.

A commercial NPT, TWEEL, was developed by Michelin for construction vehicles. Its spoke structure is the isolated curve spokes. These spokes work with other components of NPT, steel wheel, and shear band. Three regions of the force distribution happened on the spoke structure around an NPT circumference when the NPT supported a vertical load (Gasmi *et al*., 2012). They were contact, support, and free surface regions. Spokes in the contact region were not distributed load to the shear band. They just distinctly bent and formed the contact patch. The spokes in the support region would stretch to compensate for the shear band deformation and hang the hub of TWEEL (Rhyne and Cron, 2006). The spoke and shear band thicknesses then attempted to optimize the rolling resistance (Veeramurthy *et al*., 2011). Two-dimensional finite element analysis (FEA) and parametric studies were

---

*Corresponding author. e-mail: chakrit.suv@mahidol.ac.th

employed to reduce the rolling resistance of NPT with an isolated spoke. The optimization concerned the geometry and the material property of NPT. Both designed variables, shear band and spoke thicknesses, affected the response of studied parameters, only that the shear band thickness provided more effect on rolling resistance. A higher shear modulus of PU, which described the material property of spoke and shear band, also resulted in a lower rolling resistance of NPT (Veeramurthy et al., 2014). It should note that PU has low viscoelastic energy loss than rubber cause of a lower rolling resistance of NPT.

The study on spoke structures extended performing by the finite element method (FEM). Jang et al. (2012) employed topology optimization to carry out spoke patterns. The static stiffness of pneumatic tires was a goal. One of three patterns achieved by FEM and topology optimization was similar to TWEEL. Ju et al. (2012) investigated the honeycomb spokes of NPT by FEA. Three different cell expanding angles of a honeycomb spoke were designed and varied in thickness to seek the compliant spoke, which had low local stresses under microscopic uniaxial loading. They found that the lower cell expanding angle caused a higher vertical stiffness of NPT, but a higher cell angle expanding had lower local stress. The simulation results indicated that the dynamic loading generated the maximum stress value on spokes higher than the static loading. The different spoke structures comprised spoke in pairs of TWEEL, the curved spoke of Bridgestone's NPT, and the honeycomb spoke were analyzed by Aboul-Yazid et al. (2015). They found that the spoke of TWEEL had the minimum contact pressure and Von Mises stress while the vertical stiffness was highest under the same compression condition. Meng et al. (2016) proposed two types of cellular spoke structure. Three cellular-shaped spoke structures were provided for analysis by FEM. The cross arcs cell was more suitable for the spoke structure of NPT than the hexagonal and double-curved cells. The tread thickness, spring leaf thickness, spring leaf angle, spring leaf radius, and cell number of cross arcs cell spoke were varied. The simulation results indicated that the spring leaf thickness, spring leaf angle, and cell number directly affected the tire deformation, which impacted the performance of NPT. The finite element (FE) models of NPT with different honeycomb spoke geometries were carried out to study their static and dynamic behaviors (Jin et al., 2018). The maximum stress in spokes with a higher cell expanding angle was high. However, the NPT with a lower cell expanding angle was a high load-carrying capacity. In addition, the maximum stress in spokes under dynamic loading is higher than that under static loading. In the above research investigations, it can note that the finite element model of NPT for studying the structures of spoke must be assumed to be the smooth and continuous tread. Furthermore, these FE models did not build based on an authentic NPT. It may cause the impractical structures of the spoke for manufacturing.

The full NPT model according to actual TWEEL geometries was constructed and validated by Rugsaj and Suvanjumrat (2019). They obtained material properties of NPT models from the mechanical property testing of TWEEL components. They found that the vertical stiffness of NPT was too high when compared to pneumatic tires of the same size. The thickness of TWEEL's spoke then varied for the optimal vertical stiffness. The spoke thickness of 5 mm was the proper thickness of TWEEL, which provided the identical vertical stiffness to a pneumatic tire. The NPTs were further classified and found four different spoke geometries. They consisted of the isolated curve spoke, the hexagonal honeycomb spoke, the auxetic honeycomb spoke, and the polygonal cellular spoke. The FE models with different spoke structures were equivalent in weight and compared their performance. Vertical stiffness and local stress were constraints for this comparison. The results indicated that the polygonal cellular spoke was the best. After that, the numbers of polygonal cellular spokes were varied under constant weight. They found that the spoke numbers of 24 were optimal for NPT (Rugsaj and Suvanjumrat, 2020). However, these previous studies were unconcerned with the dynamic behavior of spokes. Rugsaj and Suvanjumrat (2021) studied the dynamic behavior of TWEEL. It was tested on the drum testing machine by experiment. The spoke was deformed while the NPT rolling on the drum had been captured by the high-speed video camera. They had also developed the dynamic FE model of TWEEL rolling on the drum and flat surface. The spoke deformed at various angular positions of models showed a good agreement with experimental results. TWEEL rolled on a flat plate consumed time much less than on the drum surface. Therefore, the FE model of rolling NPT on a flat plate was further used to observe the dynamic behaviors. The carrying load and rotating speed were varied to study dynamics effects. The compressive load of 20 kN and rolling speed of 15 km/hr were the limitations of this NPT because the shear stress at the interface between the shear band and outer ring of the spoke structure was higher than the allowable value. Although their studies are quietly concerned with the optimal thickness of isolated curve spokes and rolling analysis, they cannot vary the spoke numbers with the proper weight and dynamic performance of the NPT.

In the above research, the isolated curve spoke is simple than the other spoke structures. Therefore, the NPT with this spoke shape was developed and manufactured by Michelin. This research aimed to study the isolated curve spoke of TWEEL for proper weight reduction and rolling performance. The vertical stiffness of NPT, the contact patch between tread and pavement, and the maximum stress at spoke were the constraints of this study. These were also the constraints of the conventional pneumatic tires. This study has the reason that the spoke structure of NPT has high out-of-plane stiffness while the in-plane properties are

much lower. In addition, the TWEEL, which is developed for construction vehicles, is driven at a low speed. However, a high carrying load capacity and durability are needed. Therefore, the out-of-plane stiffness will not be investigated for the study. The FE models would create according to actual NPT in all its component geometries for complete analysis. These models would carry out varying the spoke numbers and thicknesses. Therefore, the vertical stiffness function, which had the numbers and thicknesses of spoke as variables, was established from the results of the empirical study. Moreover, the weight and maximum stress functions would be developed. These novel functions are reliable and practicable to design and develop suitable NPT with different isolated curve spokes for various applications.

2. FINITE ELEMENT ANALYSIS OF NON-PNEUMATIC TIRE

2.1. Finite Element Model of Vertical Stiffness Testing on TWEEL

The commercial NPT is named TWEEL, recently developed by Michelin. The TWEEL 12N16.5 SSL ALL TERRAIN is functional for supporting heavy loads in construction works. It has four main components. There are a rubber tread, a composite shear band, PU spokes, and a steel hub. All the curved spokes are in 25 pairs are aligned uniformly on a circumference of TWEEL. The TWEEL diameter and width are 860 mm and 309 mm, respectively. Figure 1 presents the TWEEL model created by MSC.marc software according to the actual TWEEL. The tread and the shear band used hexahedral elements, while the spoke used shell elements for modeling. For the shear band modeling, the homogenization approach would carry out to inserting the belt layers into a rubber layer was called a wall along the TWEEL circumference (Phromjan and Suvanjumrat, 2020). The FE model of spokes, which connected the inner to outer rings, was assumed to be a smooth thickness of 5.8 mm. The thickness of the inner and outer rings was 7 and 6 mm, respectively. The outer ring was attached to the shear band. The steel hub did not model to reduce the computation resources.

Inner ring
Spoke
Outer ring
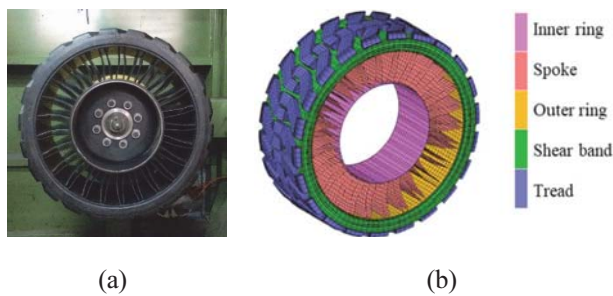Shear band
Tread

(a)   (b)

Figure 1. TWEEL 12N16.5 SSL ALL TERRAIN: (a) Actual tire; (b) Finite element model.

The material properties of TWEEL are the significant parameters for obtaining accurate FEA results. The waterjet cutting technique was performed on the components of TWEEL to prepare specimens. It cut tread to be the short circular cylinders for the compression test according to ASTM D575 standard and cut spokes to be the dumbbell specimens for the tensile test according to the ASTM D412 standard. For both testing methods, the universal testing machine (Instron 5969) was employed to carry out the stress-strain curve according to those ASTM standards. It found that the hyperelastic model is suitable material properties for modeling NPT. One of the most popular is Mooney-Rivlin hyperelastic model. Its equation writes the strain energy density per unit volume, ${}_0^t\overline{W}$, as follows:

$$ {}_0^t\overline{W} = C_1({}_0^tJ_1 - 3) + C_2({}_0^tJ_2 - 3) + \frac{1}{2}K({}_0^tJ_3 - 1)^2 \qquad (1) $$

where C_i is hyperelastic material constants and J_i is the reduced invariants which are defined as follows:

$$ {}_0^tJ_1 = {}_0^tI_1({}_0^tI_3)^{-\frac{1}{3}} \qquad (2) $$

$$ {}_0^tJ_2 = {}_0^tI_2({}_0^tI_3)^{-\frac{2}{3}} \qquad (3) $$

$$ {}_0^tJ_3 = ({}_0^tI_3)^{\frac{1}{2}} \qquad (4) $$

where ${}_0^tI_i$ is an invariant in terms of Cauchy-Green deformation tensor and K is the bulk modulus.

The governing equation will be written by the following equation (Bathe, 1997) to analyze the rubber-like material.

$$ d\,{}_0^t\overline{W} = {}_0^t\overline{S}d\,{}_0^t\varepsilon_{ij} \qquad (5) $$

where $d\,{}_0^t\overline{W}$ is the increment potential energy, ${}_0^t\overline{S}$ is the Piola-Kirchhoff stress is computed only from the displacement field, and $d\,{}_0^t\varepsilon_{ij}$ is the incremental strain.

Therefore, constants of the Mooney-Rivlin hyperelastic model for TWEEL components describe in Table 1. To prevent volumetric locking of large strain simulation, the Hermann formulation, which is the hybrid formulation of displacement and pressure, is used to analyze a rubber-like material such as tread and wall. Moreover, the generalized Maxwell's viscoelastic model (Equations (6) and (7)) describes the inelastic behavior of NPT. The viscoelastic constants represent in Table 2 (Yoo et al., 2017).

Table 1. Mooney-Rivlin constants of TWEEL components.

Components	C_1	C_2	K
Tread	1.19085	0	9,670.24
Spoke	0.5063	4.2552	42,449

Table 2. Constants of Generalized Maxwell's viscoelastic model for spoke material.

i^{th} term	τ_i	G_i
1	0.2	0.125
2	0.02	0.125
3	0.002	0.125

$$G(t) = G_0 - \sum_{i=1}^{n} G_i(1 - e^{-t/\tau_i}) \qquad (6)$$

$$\tau_i = \eta_i / E_i \qquad (7)$$

where $G(t)$ is the shear relaxation modulus, G_0 is the shear modulus at an initial condition, G_i is the ith term of the shear modulus, t is time, τ_i is i^{th} term of the relaxation time, η_i is the viscoelasticity, and E_i is the modulus of elasticity.

The flat plate pressed the TWEEL model according to the vertical stiffness testing. The friction coefficient between the TWEEL model and the rigid flat plate was 0.8. It was Coulomb's friction model used to analyze the contact model. The rigid bar elements (RBEs) linked the inner ring to a central node. The RBEs and node respectively acted like a steel hub and the axle shaft. For the stiffness testing, the center node was fixed the same as TWEEL mounting on the testing machine. When the vertical stiffness testing model processes, the rigid flat plate will move and compress the TWEEL model with a standard usage load, 14 kN, as shown in Figure 2.

2.2. Validation of FEM by Experimental Testing on the Authentic TWEEL

The tire stiffness tester (EKTRON TEK model PL-2003) was employed to perform the stiffness testing in the laboratory. The authentic TWEEL is mounted at the mounting arm of the tester and then compressed by the measurement table with a usage load of 14 kN shown in Figure 3. Furthermore, the carbon film was inserted between the NPT and table to carry out the footprint of the actual TWEEL. The load cell and displacement transducer collected the compressive force and vertical deformation of the NPT, respectively. Both testing results, experimentally and numerically, are compared by graphs and shown in

Figure 4. The experimental result indicated that the vertical stiffness of actual TWEEL was 887.89 N/mm. The vertical stiffness of FEA was 808.76 N/mm. It found that the FEA was underestimated by about 8.91 % for the vertical stiffness testing. There is a good agreement between the simulation result and the experiment result. Therefore, it confirms the FEM that is effective to model NPT and its material properties.

The footprint between the authentic TWEEL and the measurement table was represented by transferring a carbon film result. Figure 5 (a) shows the experimental footprint result. The footprint area of the authentic TWEEL was calculated (Phromjan and Suvanjumrat, 2021) and then was 350.34 cm^2. The footprint area of the FEA result is in Figure 5 (b). It was shown by the red contour. The
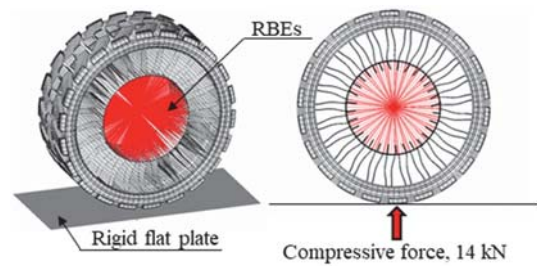

Figure 2. Finite element model of the vertical stiffness testing on NPT.

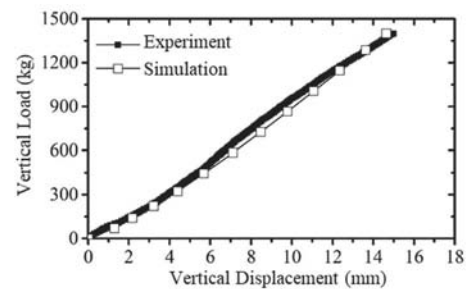Figure 3. Vertical stiffness testing of TWEEL.

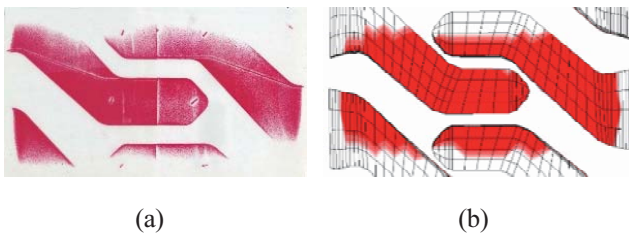Figure 4. Results of stiffness testing on TWEEL.

(a)   (b)

Figure 5. Footprint of TWEEL by (a) Experiment; (b) Simulation.

calculated footprint area was 348.34 cm^2. The simulation result was agreed well with the experimental result. It had an error of less than 0.57 %. It guarantees the same deformation between the authentic TWEEL and its FE model.

For this section, the vertical stiffness of authentic TWEEL was a lot higher than the vertical stiffness of the pneumatic tire at the same size. The vertical stiffness of the pneumatic tire, which mainly depended on inflation pressure and dimension, was estimated to be 658.17 N/mm under average operating pressure (Rugsaj and Suvanjumrat, 2019). It found that the authentic TWEEL was 1.35 times more stiffness than the pneumatic tire. It results in the motivation for adjustment of the NPT geometries, which also reduces the weight of TWEEL NPT.

3. EFFECTS ON REDUCTION OF SPOKE NUMBERS

In the previous section, the higher vertical stiffness and weight of authentic TWEEL challenged the reduction of the spoke numbers of TWEEL. The number of spoke pairs caused the higher weight of TWEEL. It also evokes the material and energy consumption for using this NPT. To optimize the TWEEL weight, it should reduce its spoke numbers. For the spoke reduction, six patterns of spoke alignment on the TWEEL circumference are proposed and shown in Figure 6. In addition, the ten and fifteen pairs of spoke patterns were two aligning styles along the circumference of TWEEL. These patterns of spoke structure were modeled by controlling the same element size. Their thickness was equal to 5.8 mm.

3.1. Static Analysis
All the FE models of TWEEL with different spoke patterns were carried out to test their vertical stiffness at the compressive load of 14 kN. The simulation results are plotted by the spoke number vs. vertical stiffness and vs. maximum stress graphs shown in Figure 7. It presented that the reduction of spoke numbers distinctly affected the vertical stiffness and maximum stress of NPT. It was also important to note that the vertical stiffness of TWEEL reduced following the decrease in spoke numbers. Furthermore, the lower spoke number would increase the
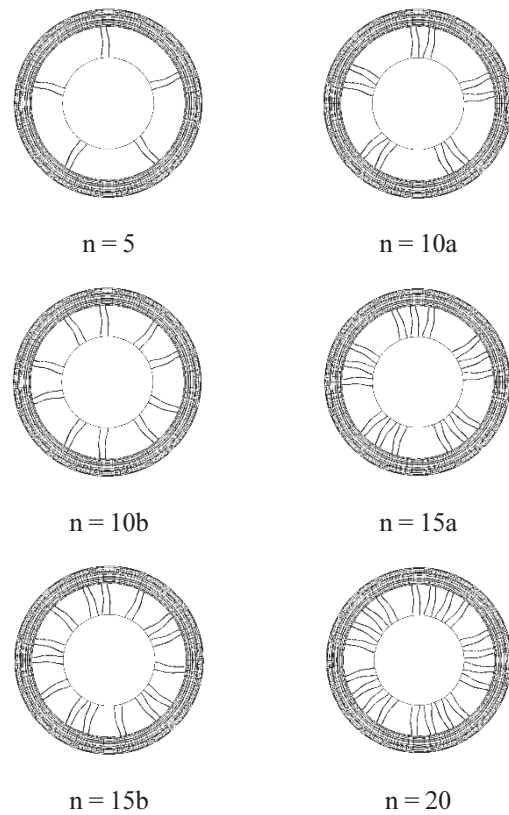

n = 5   n = 10a

n = 10b   n = 15a

n = 15b   n = 20

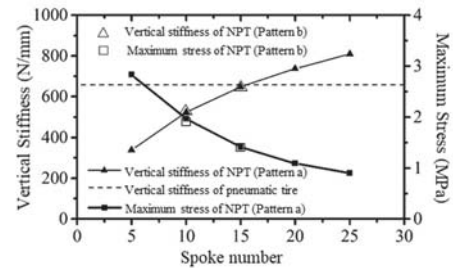Figure 6. Spoke algning patterns of TWEEL models.

Figure 7. Vertical stiffness and maximum stress of TWEEL models with different spoke patterns.

maximum stress on the deformed spokes. In addition, different patterns or positions of spoke alignment insignificantly affected the performance of TWEEL. It found that both spoke patterns of 15 pairs sequentially had different stress values and vertical stiffness values of 0.001 MPa and 0.95 N/mm. The maximum stress and vertical stiffness values between 10 spoke pairs of spoke patterns were 0.048 MPa and 2.76 N/mm, respectively. It found that the stiffness value of both TWEEL models with 15 pairs of spokes was approximate the same size as a pneumatic tire. Therefore, these TWEEL models would study further in the rolling analysis.

3.2. Dynamic Analysis

The dynamic analysis had been carried out to investigate the stress happening at the spokes of TWEEL with different spoke patterns. The rolling NPT models are in Figure 8. The preparation of these dynamic models accorded to the dynamic FE model of TWEEL in Rugsaj and Suvanjumrat (2021). The NPT models with 15 and 25 spoke pairs rotated on a rigid flat road and carried a vertical load of 14 kN. They ran with a velocity of 11 km/hr. However, these NPTs were the tire development for construction vehicles that drove at low speeds therefore effects on acceleration and braking could be neglected. The velocity was controlled for easy convergence of analysis by the gradually increased velocity value from 0 to 11 km/hr within 2 seconds. At the

(a)

(b)

(c)
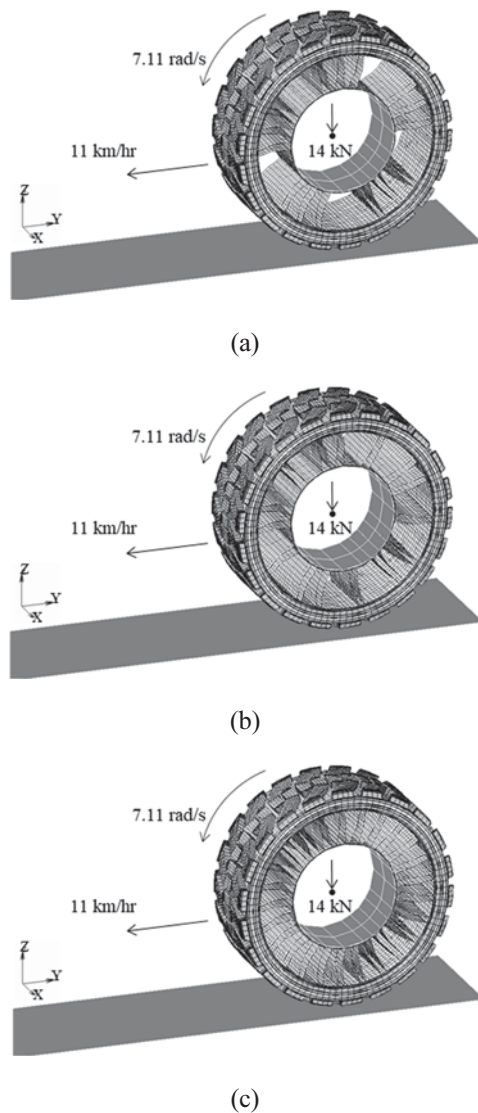
Figure 8. TWEEL models with (a) n = 15a; (b) n = 15b; (c) n = 25 pairs of spokes rolling on rigid flat road.

same time as the constant velocity setting, the NPT model rotated with an angular velocity of 7.11 rad/s. The single-step Houbolt integration was employed to solve implicit dynamic contact analysis in this study. The equilibrium equation of linear dynamics for the analysis of rolling NPT models is written as follows:

$$M\ddot{x} + C\dot{x} + kx = F \tag{8}$$

where M, C, and k are the mass, viscous damping, and stiffness matrix, respectively. x is the displacement vertor and F is the applied load vector.

According to the single-step Houbolt algorithm, the equation of motion gives as follows:

$$x(t_{n+1}) = x(t_n) + \Delta t \dot{x}(t_n) + \beta \Delta t^2 \ddot{x}(t_n) + \beta_1 \Delta t^2 \ddot{x}(t_{n+1}) \tag{9}$$

$$\dot{x}(t_{n+1}) = \dot{x}(t_n) + \beta \Delta t \ddot{x}(t_n) + \beta \Delta t^2 \dddot{x}(t_{n+1}) \tag{10}$$

where t is time, while β and β_1 are constant. In this research, in order to get stability results, the values of β and β_1 are -1/2 and 1, respectively.

The dynamic simulation results indicate that the maximum stress of 3 spoke patterns will always occur at spokes in the support region, opposite to the contact side, of the NPT model (Figure 9). It should note that the tension force caused the maximum stress. Furthermore, these spokes would encounter cyclic tension-compression loading. Simulation results also indicated that the stress level of spokes under dynamic load was usually higher than that under static load. To describe the effect of spoke alignment clearly, Figure 10 sequentially present the non-uniform response of rolling TWEEL models with different spoke patterns step by step. The maximum stress happened on the 15a spoke pattern of the TWEEL distinctly depending on the spoke alignment. When these spokes were in the center of the support region, their maximum stress value was low. Inversely, if the opposite side of the contact region was empty with spokes in there, the maximum stress value increased. In the same manner, it could observe that the 15b spoke pattern provided a more uniform response. It was because the angle of the spoke gap was smaller.

The maximum stress at spoke of both 15 pairs of spoke aligning patterns is compared in time history with the original one as shown in Figure 10 (c). Both reduced-spoke TWEEL models were any insignificant difference in maximum stress occurring at spokes while they rotated on the road. Its stress value could represent the durability of spokes to the fatigue failure. The average maximum stress value of both reduced-spoke TWEEL models was more than the original TWEEL model 1.51 times. Moreover, the
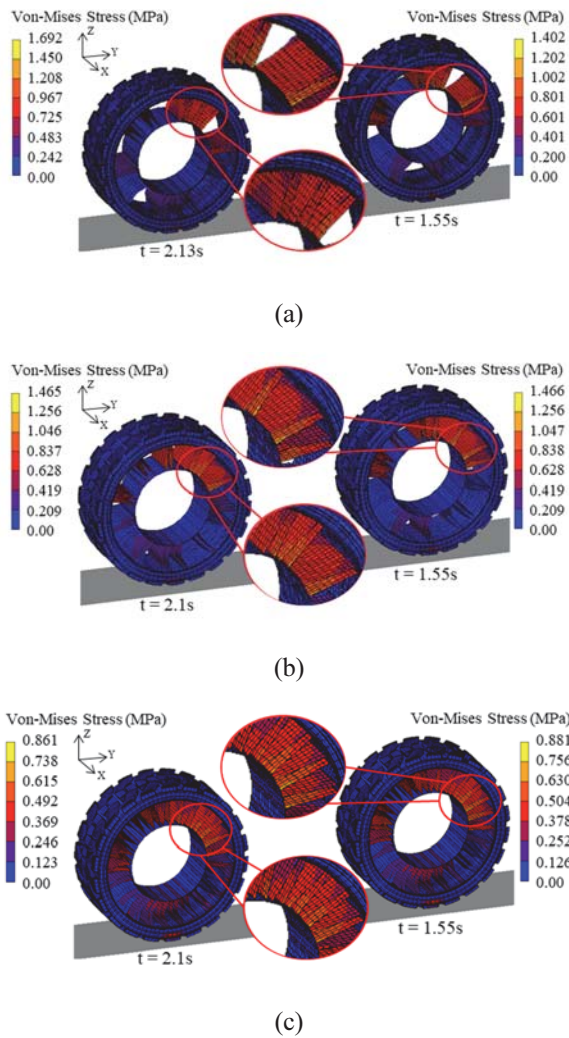
(a)

(b)

(c)

Figure 9. Deformation and maximum stress of TWEEL models with (a) n = 15a; (b) n = 15b; (c) n = 25 pairs of spokes rolling on rigid flat road.

(a)

(b)

(c)

Figure 10. Maximum stress at (a) n = 15a; (b) n = 15b spoke TWEEL; (c) 2 reduced-spoke and original TWEEL.

average maximum stress under the dynamic case was higher than under the static case at a similar value in every type of spoke alignment, which is higher than under the static case 1.09 times on average. Figure 11 shows the impact force response of the ground on the rolling NPTs. It found an infinitesimally different frequency of the impact force signal between both reduced-spoke TWEEL. The peak-to-peak of impact force, which was occurred by the rolling original TWEEL model, was the highest vibrating value. It found that the reduced-spoke models obtained the lowest value of tire vibrating. It should note that higher weight and stiffness, which caused more vibration, belonged to the original TWEEL. It means that the reduced-spoke TWEEL has a more comfortable riding on the roads. Consequently, it can summarize that the lightweight of TWEEL is appropriate for the suspension of construction vehicles (Phromjan and Suvanjumrat, 2018).
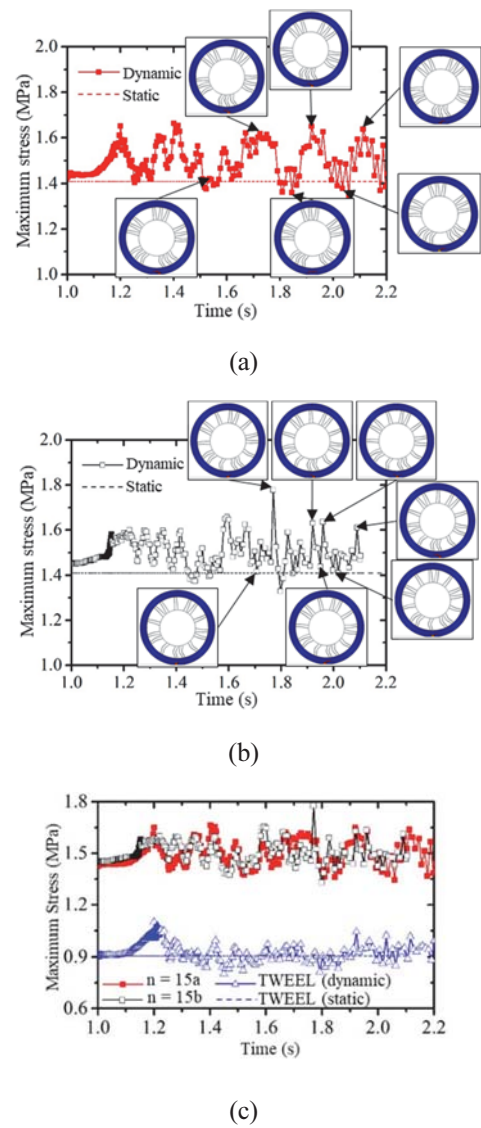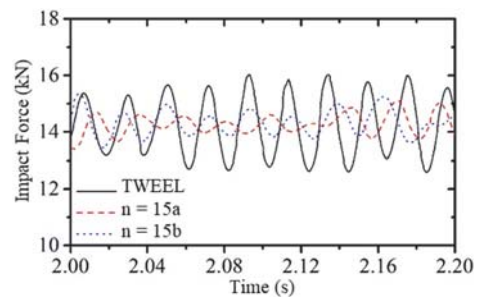

Figure 11. Impact force between rolling NPTs and road.

3.3. Verification of the Reduced-Spoke TWEEL
The water jet cutting technique has used to cut the original

spokes of TWEEL into the 15b spoke pattern for the vertical stiffness testing is shown in Figure 12. This reduced-spoke TWEEL had been performed by the tire stiffness tester in the same conditions as described in the previous section. It found that the vertical stiffness of reduced-spoke TWELL was 650.02 N/mm. It also noted that the vertical stiffness of reduced-spoke TWEEL was lower than the original TWEEL. However, this value was close to the stiffness of the same size pneumatic tires. The experimental results compared against the FEA results are shown in Figure 13. The average error of FEA was less than 0.30 %. Therefore, it can accept that the FE model of reduced-spoke TWEEL is reliable to study the effects of spoke numbers on NPT performances in the next section. Furthermore, the processing time of the static model was much shorter than the dynamic model. Therefore, the vertical stiffness testing model would suggest studying the effect of various spoke geometries of the NPT models.

4. GEOMETRIC STUDY ON SPOKES OF NPT

4.1. Spoke Alignment

As mentioned above, the reduced-spoke TWEEL, which had a gap angle between pairs of spokes uniformly, was less vibration. Therefore, the uniform spokes alignment was the consequential requirement to study the effects of spokes on NPT performances. The FE models of NPT with uniform spokes alignment were carried out by re-arranging these isolated curve spokes on the NPT's circumference. The angle between pairs of spokes was equal. Consequently, there are 4 NPT models with new spoke patterns in Figure 14. Therefore, all NPT models included the original TWELL with uniformly spoke aligning would simulate the vertical stiffness testing in the next section.

4.2. Vertical Stiffness

The most significant parameter is used to describe the carrying load capability of tires is the deformation of the tire. The accurate FE model can provide those detail not only deformation but stress distribution in every component of NPT also. Figure 15 shows the color contour of deformation which happens to the NPT. The maximum displacement of spokes was in the contact region that was buckling. These spokes were bent and did not apply load to the shear band. Inversely, the spokes at the opposite side of the contact region, wherein the region was called the support region, were stretched due to the tension force (Gasmi *et al.*, 2012). The maximum stress in each region can represent distinctly by the color contour shown in Figure 16. In addition, it was found that the maximum stress value occurred at spokes that hung the hub in the support region. The spoke structure, which was studied in this research, was classified as a curved isolated spoke structure. When carrying load was applied on the NPT,

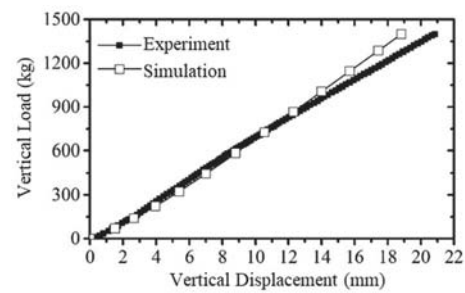Figure 12. Stiffness testing on the authentic TWEEL with the reduced-spoke case n = 15b.

Figure 13. Comparison of stiffness testing results of the reduced-spoke TWEEL between experiment and simulation.

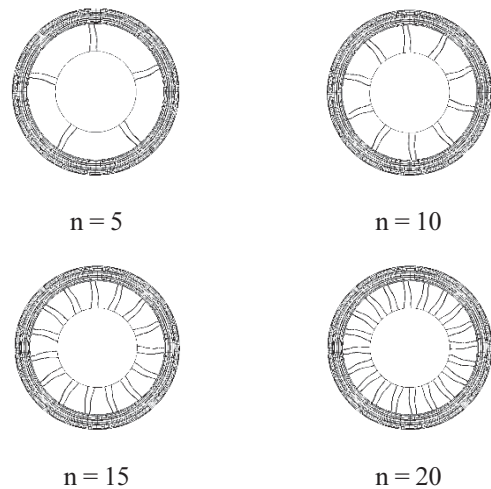n = 5   n = 10

n = 15   n = 20

Figure 14. Four novel NPT models with different spoke patterns.

spokes in the contact region underwent bending and buckling modes. Therefore, the carrying load was less supported by spokes in this region. However, spokes in the support region were stretched by hanging the load via the hub instead. Thus, the maximum stress was observed on
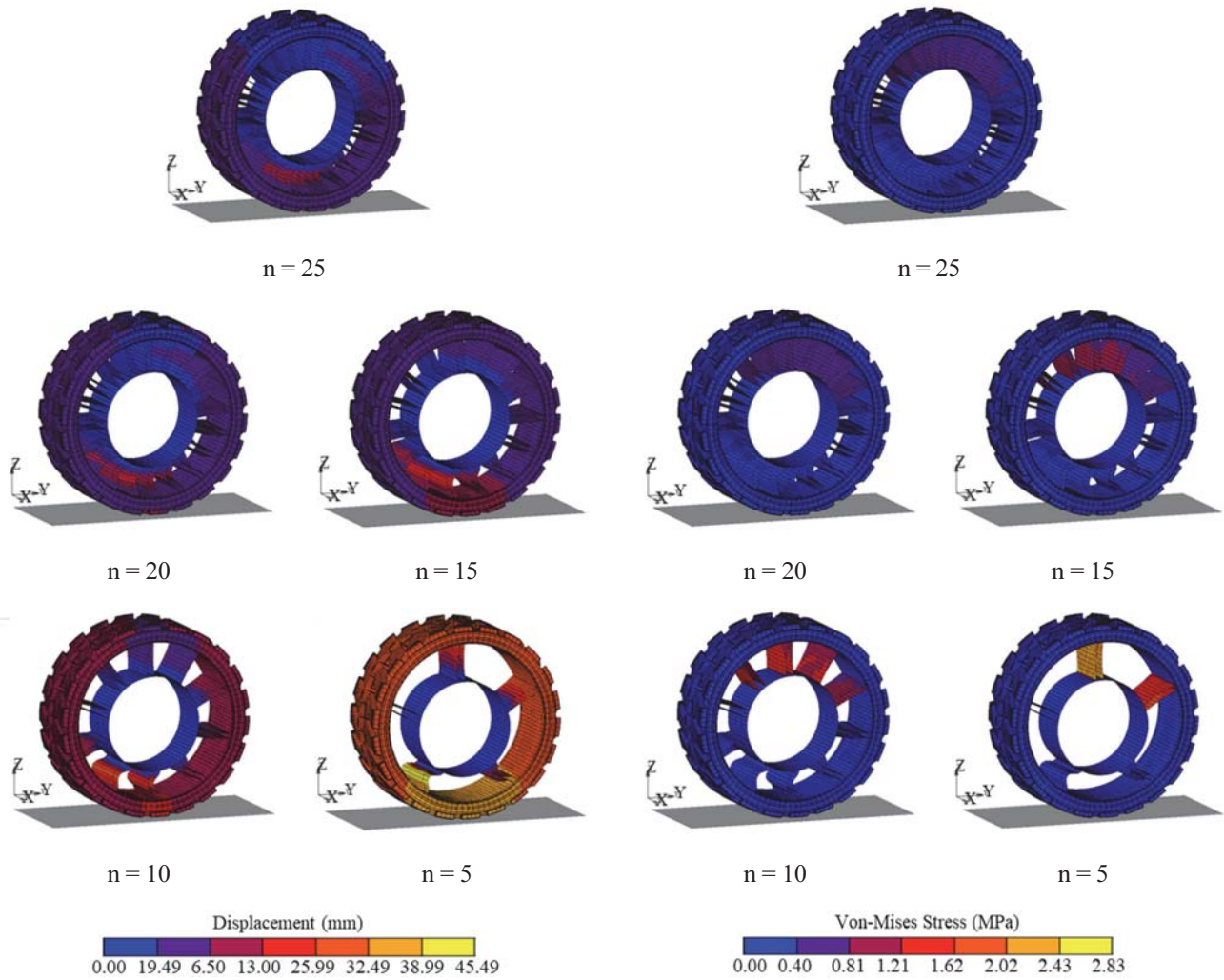
n = 25

n = 20   n = 15

n = 10   n = 5

Displacement (mm)

0.00   19.49   6.50   13.00   25.99   32.49   38.99   45.49

Figure 15. Deformation of the NPT models under the compressive force of 14 kN.

n = 25

n = 20   n = 15

n = 10   n = 5

Von-Mises Stress (MPa)

0.00   0.40   0.81   1.21   1.62   2.02   2.43   2.83

Figure 16. Maximum stress on spoke of the NPT models under the compressive force of 14 kN.

spokes in this region. The simulation results distinctively represented both types of the spoke working by color contours of displacement and stress distribution. Spokes in the support region of the NPT model with the lowest spoke number were extremely stretched that the high stress occurred. Inversely, a more spoke NPT was deformed less than the lower number of spokes because the tension force separated into many spokes of the support region. This effect decreased gradually in the free surface region, where the force distribution was negligible. It was because there was neither tension nor contact. For the NPT model with the spoke number of 5, each pair of spoke alignment seemed too far from each other. It found that the spokes were not in the free surface region. The cause of the force transmission suddenly skipped from high tension to high compression resulting in the concentrated stress happening at spokes.

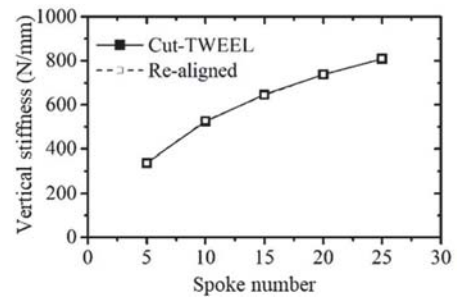Figure 17 shows the compared results between the

Figure 17. Comparison of vertical stiffness of different spoke alignments.

uniformly aligned spoke TWEEL and previous reduced-spoke TWEEL. It found that the uniformly aligned spoke models gave the same results as the reduced-spoke TWEEL model. It should note that the angle between one pair of

spokes, which is less than 28.8 degrees, does not affect the vertical stiffness of NPT. Therefore, these FE models of the uniformly aligned spoke of TWEEL were further used to study the effects on TWEEL's geometries. Furthermore, the uniform alignment of spokes is practical to manufacture proper TWEEL NPTs in the future.

4.3. Footprint Area

This section presented the effects on footprint area, which described the contact efficiency of NPT. The simulation results of the NPT model with different numbers of spokes under the compressive load indicated that the footprint area was not affected by the number of spokes. As mentioned in the previous section, the deformation was principally found at spoke because its function was the resilient part. While, the shear band was sturdy to maintain the NPT shape by insertion of belt layers which provided a low stiffness in the radial direction and high stiffness in the circumferential direction (Marcin et al., 2019). Figure 18 shows the red color contour of the contact area happening on the tread of NPT at the spoke thickness of 5.8 mm. The simulation results showed that the footprint area was insignificantly different by changing the number of spokes. In all the cases of FEA, the color contour happened the same, and the footprint area was 348.34 cm^2. It should note that the vertical displacement of NPT generally occurred on its spoke.

4.4. Spoke Thickness

To study the effects of spoke thicknesses on the NPT, the thickness of spokes was uniform and varied to 4, 4.5, 5, 5.8, 6, 6.5, 7, and 7.5 mm. Meanwhile, the thickness of the inner and outer rings was 7 and 6 mm, respectively. The simulation results of the vertical stiffness testing plot graphs are in Figure 19. It found that the vertical stiffness of the NPT models increased in a polynomial trend by the increase of spoke numbers when considering each thickness of spokes. Furthermore, the vertical stiffness also was a logarithmic increase when increasing the spoke thicknesses. Figure 20 shows the decrease of stress when increasing spoke numbers. To take the spoke durability into account, while the yield stress of the spoke was 6 MPa, the maximum stress value of the NPT model with the spoke pairs of 5 is too close to the limit than the other spoke number. The safety factor of these spokes was maximum only at 2.42. Therefore, they resulted in the unsafety of design because the acceptable value of safety was 2. These numbers of spoke alignment for NPT are unsuggested for manufacturing. To be convenient to design spoke patterns of NPT further, the formulations used to calculate the suitable spoke numbers and thicknesses are required. Therefore, these formulas will be established in the next section to use instead of FEA.

n = 20   n = 15
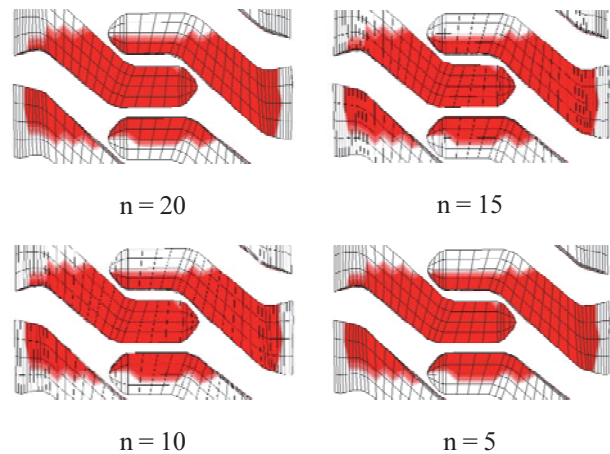
n = 10   n = 5

Figure 18. Contact area of uniformly aligned spoke NPTs due to the compressive force of 14 kN.
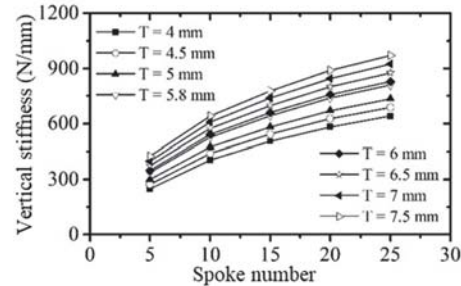

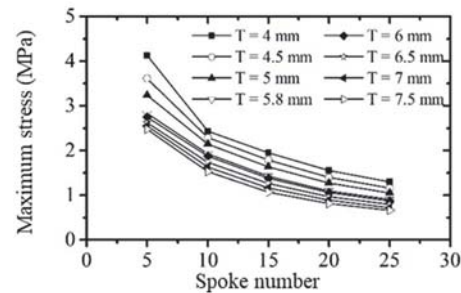Figure 19. Vertical stiffness of NPT models with various numbers and thicknesses of spokes.

Figure 20. Maximum stress of NPT models with various numbers and thicknesses of spokes.

5. FUNCTIONS IN THE DESIGN OF NPT

Because the vertical stiffness of NPT is the significant performance of the NPT for construction vehicles, its function would propose for the NPT design. The Cowper-Symonds model, which successfully fitted two variables (Suvanjumrat and Puttapitukporn, 2011), was

employed to the fitting of nonlinear behavior of the NPT's geometries. The general form of the Cowper-Symonds model writes as TWEEL's vertical stiffness (K_z) in the function of number (n) and thickness (T) of spokes as shown in the following equations.

$$\frac{K_z(n,\mathrm{T})}{K_{z,\mathrm{T}=4}(n)} = 1 + \left(\frac{T}{D}\right)^{1/P} \quad (11)$$

where $K_z(n,\mathrm{T})$ is the TWEEL's vertical stiffness function of number and thickness of spokes, $K_{z,\mathrm{T}=4}(n)$ is the TWEEL's vertical stiffness function of the spoke number at the spoke thickness of 4 mm, while D and P are the contants of this function.

Next, Equation (11) can be rewritten as follows:

$$\frac{K_z(n,\mathrm{T})}{K_{z,\mathrm{T}=4}(n)} - 1 = \left(\frac{T}{D}\right)^{1/P} \quad (12)$$

Equation (12) transforms into the logarithms function. Therefore it can rewrite as follows:

$$\log\left(\frac{K_z(n,\mathrm{T})}{K_{z,\mathrm{T}=4}(n)} - 1\right) = \log\left(\frac{T}{D}\right)^{1/P} \quad (13)$$

, or

$$\log\left(\frac{K_z(n,\mathrm{T})}{K_{z,\mathrm{T}=4}(n)} - 1\right) = \left(\frac{1}{P}\right)\log T - \left(\frac{1}{P}\right)\log D \quad (14)$$

As mentioned above, D and P are the constants. Equation (14) forms a linear equation. Consequently, a single variable linear regression method uses to determine D and P by substituting the data from FEA as presented in Table 3 into Equation (14). The D and P constants eventually are 8.39 and 0.27, respectively.

As presented in the previous section, the vertical stiffness was related to the spoke numbers in a polynomial trend. For the TWEEL NPT, the vertical stiffness function of spoke numbers at the thickness of 4 mm is written as shown in Equation (15).

$$K_{z,\mathrm{T}=4} = -0.622n^2 + 37.98n + 77.55 \quad (15)$$

Equation (15) substitutes into Equation (11), it can be rearranged as follows:

$$\frac{K_z}{-0.622n^2 + 37.98n + 77.55} = 1 + \left(\frac{T}{8.39}\right)^{1/0.27} \quad (16)$$

Table 3. Vertical stiffness of the NPT with the various numbers of spokes and thicknesses.

Spoke thickness (T, mm)	Vertical stiffness (K_z, N/mm)				
	$n = 5$	$n = 10$	$n = 15$	$n = 20$	$n = 25$
4	247.53	404.95	504.08	582.66	641.42
4.5	273.25	439.11	54304	625.57	687.20
5	298.49	472.90	581.72	668.45	733.49
5.8	338.38	526.62	643.72	738.35	808.76
6	348.68	540.04	659.35	755.88	827.77
6.5	374.07	573.59	698.61	799.99	875.30
7	399.53	607.13	738.04	844.31	922.64
7.5	425.11	640.57	777.28	888.31	969.53

Therefore, the TWEEL's vertical stiffness function can eventually be written as follows:

$$K_z = (-0.622n^2 + 37.98n + 77.55)\left(1 + \left(\frac{T}{8.39}\right)^{\frac{1}{0.27}}\right) \quad (17)$$

The vertical stiffness values could obtain by calculating with Equation (17). They compare against the FEA results are shown in Figure 21. The comparison results indicated that the calculated vertical stiffness values by the TWEEL's vertical stiffness function had a good agreement with simulation results. The average error was less than 3.69 %. The optimal spoke numbers and thicknesses of TWEEL determine by defining the limits of vertical stiffness at 658.17 N/mm as the standard vertical stiffness of a pneumatic tire (dash line). It should note that the spoke thicknesses and numbers on the dashed line are reasonable to be the optimal spoke pattern of NPT. In addition, the vertical stiffness can increase reasonably to design proper NPT for other applications.
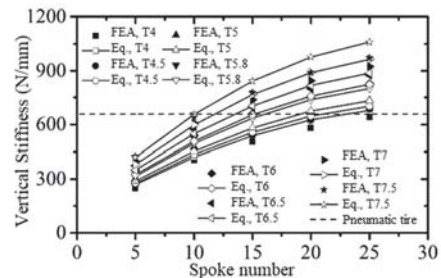

Figure 21. Comparison of the vertical stiffness between the TWEEL's vertical stiffness function and FEA.

Table 4. Weight of the spokes with various numbers and thicknesses.

Spoke thickness (T, mm)	Weight (W, kg)				
	n = 5	n = 10	n = 15	n = 20	n = 25
4	1.64	3.27	4.90	6.54	8.17
4.5	1.84	3.68	5.52	7.36	9.20
5	2.04	4.09	6.13	8.17	10.22
5.8	2.37	4.74	7.11	9.48	11.85
6	2.45	4.90	7.36	9.81	12.26
6.5	2.66	5.31	7.97	10.63	13.28
7	2.86	5.72	8.58	11.44	14.30
7.5	3.07	6.13	9.20	12.26	15.33

Table 5. Maximum stress at spokes with various numbers and thicknesses.

Spoke thickness (T, mm)	Maximum stress (σ_{max}, MPa)				
	n = 5	n = 10	n = 15	n = 20	n = 25
4	4.128	2.430	1.949	1.549	1.293
4.5	3.609	2.287	1.784	1.399	1.160
5	3.240	2.146	1.636	1.269	1.053
5.8	2.830	1.921	1.426	1.096	0.906
6	2.749	1.869	1.378	1.057	0.873
6.5	2.621	1.741	1.265	0.967	0.794
7	2.551	1.629	1.163	0.888	0.723
7.5	2.475	1.523	1.067	0.815	0.659

The errors of this function would find in the high number and thickness of spoke a little. The high value of vertical stiffness affected the deformation and the compensation of the shear band. Therefore, it was a cause of the error. It can observe that the contact patch less changed at the higher number and thickness of spokes. The spokes in the contact region were a very rigid cause of the deformation of tread happening instead.

As mentioned above, the decrease in spoke numbers induced the reduction of NPT weight. It could also reduce energy consumption for driving vehicles with NPTs. To know the reduced weight, Table 4 describes the weight of each spoke thickness and number. The relationship between the vertical stiffness and the weight (W) can be developed and written by Equation (18). This function has a good agreement with FEA and has a coefficient of determination (R^2) of 0.98.

$$W = (2 \times 10^{-5})K_z^2 + 0.0012K_z + 0.2263 \qquad (18)$$

In the same way, the maximum stress at the spoke changes by various geometries of spoke as presented in Table 5. According to the simulation results, the relationship between the vertical stiffness and the maximum stress (σ_{max}) will write by Equation (19). The R^2 of the stress function is 0.98.

$$\sigma_{max} = (6 \times 10^{-6})K_z^2 - 0.0109K_z + 6.0615 \qquad (19)$$

For example, the spoke weight can reduce to 32.11 % from the original spoke weight when this NPT is manufactured by designing a spoke number of 10 and a thickness of 7.5 mm. Meanwhile, the vertical stiffness of the NPT with these geometries is 656 N/mm which is still close to the average vertical stiffness of equal size pneumatic tire. The maximum stress will increase from the original TWEEL

of 64.79 %. However, the safety factors of the novel designed NPT under static and dynamic analysis were 4.02 and 3.69, respectively. In addition, these spoke geometries are easier to manufacture because of the more simple spoke structure. It is also profitable when the novel NPT mold is cheaper than the old NPT because it reduces the complexity. Furthermore, the NPT can produce for various applications such as a wheelchair, trucks, military vehicles, space rovers, earthmovers with suitable spoke geometries using these proposed functions.

6. CONCLUSION

The NPT was created to use with construction vehicles for a high load capability had been studied in this research. The FE model of NPT was performed according to the actual NPT, which is named TWEEL. The material properties of each authentic TWEEL component were determined by standard testing. Therefore, the hyperelastic material model could obtain from the experiment for the FEM. The vertical stiffness testing was performed with the authentic NPT to validate the FE model. It found that the simulation results had good agreement with the experiment. The average error of FEA for vertical stiffness and footprint area was less than 8.91 % and 0.57 %, respectively.

The geometric study of spokes was a significant requirement to reduce energy and material consumption for using NPTs. The reduced-spoke NPTs were modeled according to TWEEL geometries, which cut spokes from 25 to 5 pairs with an interval of 5 pairs of spokes. After the vertical stiffness simulation of these reduced-spoke NPT models, one model was carefully selected for validation. The waterjet cutting technique was used to cut the authentic TWEEL spokes into 15 pairs of spoke according to the selected FE model. The deformation of reduced-spoke TWEEL was a good agreement between experiment and simulation. The FEA had an average error of less than

0.30 %. In addition, it found that the angle between spoke pairs was less than 28.8 degrees and did not affect the vertical stiffness of NPT. This reduced-spoke model was further performed the dynamic analysis. It found that the lower spoke number could reduce the vibration of rolling TWEEL. Furthermore, the maximum stress would happen on the spokes in the support region. However, its average value was more than the static analysis of 1.09 times.

The effects on NPT performance with various spoke numbers and thicknesses were studied. The spokes of the NPT model are uniformly aligned around its circumference. There were five patterns of spoke alignment. These NPT models with uniform spoke alignment were performed the vertical stiffness testing. It found that the spoke alignment unaffected the vertical stiffness of NPT.

The vertical stiffness of NPTs was changed in polynomial trend by various numbers of spokes while the thickness of spokes was constant. The less spoke brought a high deformation to spokes in the contact region and caused high stress at spokes in the support region. On the other hand, the footprint area of the NPT model, which accorded to TWEEL geometry, was not affected by the number of spokes. For the effects of spoke thickness, the vertical stiffness of NPT was in a logarithmic trend while the number of spokes was constant.

The vertical stiffness function of NPT in terms of the number and thickness of spoke had been developed to use instead of the FEM. This function provided consistent results when compared to FEA results. There was an average error of 3.69 % for the comparison, which eliminated all of the complexity of the FEM. Moreover, the weight and maximum stress of spoke in terms of the vertical stiffness had been also developed. These functions would utilize to support the NPT design. For the case study, the NPT with a spoke number of 10 pairs could reduce weight to 32.11 %, while its vertical stiffness and safety factors were 656 N/mm and 3.69, respectively. Therefore, functions of the NPT design can optimize the numbers and thicknesses of spokes for suitable applications. They also reduce resource consumption to manufacture NPTs in the future.

REFERENCES

Aboul-Yazid, A. M., Emam, M. A., Shaaban, S. and Nashar, E. (2015). Effect of spokes structures on characteristics performance of non-pneumatic tires. *Int. J. Automotive and Mechanical Engineering* **11**, **1**, 2212–2223.

Bathe, K. J. (1997). *Finite Element Procedures.* Prentice Hall. London, UK.

Bitzer, T. N. (1997). *Honeycomb Technology Materials, Design, Manufacturing, Applications and Testing*. Springer-Science+Business Media, New York, NY, USA.

Gasmi, A., Joseph, P. F., Rhyne, T. B. and Cron, S. M. (2012). Development of a two-dimensional model of a compliant non-pneumatic tire. *Int. J. Solids and Structures* **49**, **13**, 1723–1740.

Jang, G. I., Sung, H. Y., Yoo, J. E. and Kwak, M. B. (2012). Pattern design of a non-pneumatic tyre for stiffness using topology optimization. *Engineering Opimization* **44**, **2**, 119–131.

Jin, X., Hou, C., Fan, X., Sun, Y., Lv, J. and Lu, C. (2018). Investigation on the static and dynamic behaviors of non-pneumatic tires with honeycomb spokes. *Composite Structures*, **187**, 27–35.

Ju, J., Kim, D-M. and Kim, K. (2012). Flexible cellular solid spokes of a non-pneumatic tire. *Composite Structure* **94**, **8**, 2285–2295.

Marcin, Z., Jerzy, J. and Hryciow, Z. (2019). Nunerical research of selected features of the non-pneimatic tire. *AIP Conf. Proc.*, **2078**, 020027.

Meng, F., Lu, D. and Yu, J. (2016). Flexible cellular structures of a non-pneumatic tire. *Int. Design Engineering Technical Conf. Computers and Information in Engineering Conf. (IDETC-CIE)*, Charlotte, North Carolina, USA.

Phromjan, J. and Suvanjumrat, C. (2018). Vibration effect of two different tires on baggage towing tractors. *J. Mechanical Science and Technology* **32**, **4**, 1539–1548.

Phromjan, J. and Suvanjumrat, C. (2020). The modification of steel belt layer of airless tire for finite element analysis. *IOP Conf. Series: Materials Science and Engineering*, **773**, 012047.

Phromjan, J. and Suvanjumrat, C. (2021). Development of solid tire model for finite element analysis of compressive loading. *Songklanakarin J. Science and Technology* **43**, **1**, 229–236.

Rhyen, T. B. and Cron, S. M. (2006). Development of non-pneumatic wheel. *Tire Science and Technology* **34**, **3**, 150–169.

Rugsaj, R. and Suvanjumrat, C. (2019). Proper radial spokes of non-pneumatic tire for vertical load supporting by finite element analysis. *Int. J. Automotive Technology* **20**, **4**, 801–812.

Rugsaj, R. and Suvanjumrat, C. (2020). Study of geometric effects on nonpneumatic tire spoke structures using finite element method. *Mechanics Based Design of Structures and Machines*, 1–21.

Rugsaj, R. and Suvanjumrat, C. (2021). Dynamic finite element analysis of rolling non-pneumatic tire. *Int. J. Automotive Technology* **22**, **4**, 1011–1022.

Sim, J., Hong, J., Cho, I. and Lee, J. (2021). Analysis of vertical stiffness characteristics based on spoke shape of non-pneumatic tire. *Applied Sciences*, **11**, 2369.

Suvanjumrat, C. and Puttapitukporn, T. (2011).

Determination of drop-impact resistance of plastic bottles using computer aided engineering. *Kasetsart J.: Natural Science* **45**, **5**, 932–942.

Veeramurthy, M., Ju, J., Thompson, L. L. and Summers D. J. (2014). Optimisation of geometry and material properties of a non-pneumatic tyre for reducing rolling resistance. *Int. J. Vehicle Design* **66**, **2**, 193–216.

Veeramurthy, M., Ju, J., Thompson, L. L. and Summers, J. D. (2011). Optimization of a non-pneumatic tire for reduced rolling resistance. *Int. Design Engineering Technical Conf. Computers and Information in Engineering Conf. (IDETC-CIE)*, Washington DC, USA.

Yoo, S., Uddin, M. S., Heo, H., Ju, J. and Choi, S. (2017). Thermoviscoelastic modeling of a nonpneumatic tire with a lattice spoke. *Proc. Institution of Mechanical Engineering, Part D: J. Automobile Engineering* **231**, **2**, 241–252.